BULLET: Jurnal Multidisiplin Ilmu
Volume 01, No. 03, Juni-Juli 2022
ISSN 2829-2049 (media online)
Hal 539-552

Simulation of a two link planar anthropomorphic manipulator

Syed Muhammad Asif

Queen Mary University of London

sm.asif@hotmail.com

Abstract

Mathematical modelling of the dynamics of a two-link planar anthropomorphic manipulator has been established to obtain the simulations on MATLAB/SIMULINK. After successful simulation, results were then used to determine the factors that govern the performance of the manipulator. It also enabled to analyze the extent to which a particular factor governed the performance or output of the robot. After the analysis, it was apparent that increase in step size increased the accuracy of the results. Moreover, it was also observed that increasing mass of the tip increased the torque input to the system.

Keywords: Two-link planar manipulator, anthropomorphic robot, mathematical modeling, MATLAB/SIMULINK, simulation, performance analysis, step size, torque input, tip mass, robotic dynamics.

INTRODUCTION

Robotic manipulators have various applications from manufacturing to healthcare to domestic uses. Most of the products that are used or encountered involves a robotic manipulator. Their ability to perform better in many cases than humans have resulted in greater use and improved life standards [1]. Two-link manipulators resemble a human hand and for this particular reason they are very useful in many real life applications. Studying a two-link manipulator allows researchers to study and understand the complex movement of human hand [2].

Two-link manipulators are two degree of freedom robots. Kinetic and potential energies are defined and derived which are then used to develop Euler-Lagrange equation. Torques applied to each link is then defined by Euler-Lagrange equation [3].

AIM

The aim of this report is to investigate the factors governing the performance of a simple servo-controlled two link robot manipulator and relate these to basic analytical techniques [4].

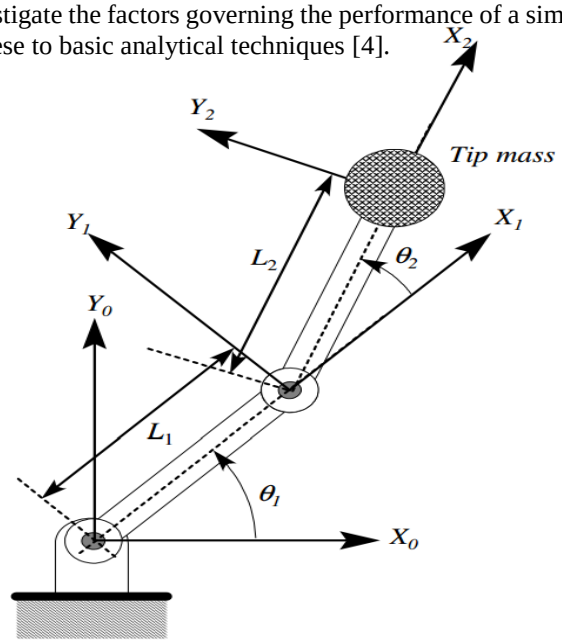

Figure 1: Two-link planar anthropomorphic manipulator [1]

BULLET: Jurnal Multidisiplin Ilmu
Volume 01, No. 03, Juni-Juli 2022
ISSN 2829-2049 (media online)
Hal 539-552

BACKGROUND THEORY

MATHEMATICAL MODELLING

General equations of motion of a two link manipulator can be written as;

$$\dot{\theta}_1 = \omega_1$$

$$\dot{\theta}_2 = \omega_1 - \omega_2$$

$$\begin{bmatrix} I_{11} & I_{12} \\ I_{21} & I_{22} \end{bmatrix} \begin{bmatrix} \dot{\omega}_1 \\ \dot{\omega}_2 \end{bmatrix} + (m_2 L_{2cg} + ML_2) L_2 \sin(\theta_2) \begin{bmatrix} \omega_1^2 - \omega_2^2 \\ \omega_1^2 \end{bmatrix} + g \begin{bmatrix} \Gamma_1 \\ \Gamma_2 \end{bmatrix} = \begin{bmatrix} T_1 \\ T_2 \end{bmatrix}$$

Where; m_i, L_i, L_{icg} and k_{icg} are the mass, length, the position of the centre of gravity with reference to the i[th] joint and radius of gyration about the centre of gravity of the i[th] link.

$$I_{11} = m_1\left(L_{1cg}{}^2 + k_1{}^2\right) + m_2 L_1{}^2 + ML_1{}^2 + cos\theta_2 L_1 (m_2 L_{2cg} + ML_2)$$

$$I_{12} = m_2\left(L_{2cg}{}^2 + k_2{}^2\right) + ML_2{}^2 + cos\theta_2 L_1 (m_2 L_{2cg} + ML_2)$$

$$I_{21} = cos\theta_2 L_1 (m_2 L_{2cg} + ML_2)$$

$$I_{22} = m_2 (L_{2cg}{}^2 + k_2{}^2) + ML_2{}^2$$

$$\Gamma_1 = cos\theta_1\left(m_1 L_{1cg} + m_2 L_1 + ML_1\right) + cos(\theta_1 + \theta_2)\left(m_2 L_{2cg} + ML_2\right)$$

$$\Gamma_2 = cos(\theta_1 + \theta_2)\left(m_2 L_{2cg} + ML_2\right)$$

Because of the fact that the links used are same, following assumptions are made;

1) $M = \mu$
2) $m_1 = m_2 = 1$
3) $L_{1cg} = L_{2cg} = \frac{1}{2}$
4) $k_1^2 = k_2^2 = \frac{1}{12}$
5) $L_1 = L_2 = 1$
6) $\mu = \frac{M}{m}$

$$\dot{\theta}_1 = \omega_1,$$
$$\dot{\theta}_2 = \omega_2 - \omega_1$$

$$\begin{bmatrix} \left(\mu + \frac{4}{3}\right) + \left(\mu + \frac{1}{2}\right) cos\theta_2 & \left(\mu + \frac{1}{3}\right) + \left(\mu + \frac{1}{2}\right) cos\theta_2 \\ \left(\mu + \frac{1}{2}\right) cos\theta_2 & \mu + \frac{1}{3} \end{bmatrix} \begin{bmatrix} \dot{\omega}_1 \\ \dot{\omega}_2 \end{bmatrix} = -\left(\mu + \frac{1}{2}\right) sin\theta_2 \begin{bmatrix} \omega_1^2 - \omega_2^2 \\ \omega_1^2 \end{bmatrix} + \begin{bmatrix} T_1/mL^2 \\ T_2/mL^2 \end{bmatrix}$$

The above equation can also be expressed as;

$$\Delta(\mu) \begin{bmatrix} \dot{\omega}_1 \\ \dot{\omega}_2 \end{bmatrix} = \begin{bmatrix} \mu + \frac{1}{3} & -\left(\mu + \frac{1}{3}\right) - \left(\mu + \frac{1}{2}\right) cos\theta_2 \\ -\left(\mu + \frac{1}{2}\right) cos\theta_2 & \mu + \frac{4}{3} + \left(\mu + \frac{1}{2}\right) cos\theta_2 \end{bmatrix} \left[\begin{bmatrix} T_1/mL^2 \\ T_2/mL^2 \end{bmatrix} - \left(\mu + \frac{1}{2}\right) sin\theta_2 \begin{bmatrix} \omega_1^2 - \omega_2^2 \\ \omega_1^2 \end{bmatrix} \right]$$

Where;

$$\Delta(\mu) = \left(\frac{7}{36} + \frac{2}{3}\mu + \left(\mu + \frac{1}{2}\right)^2 \sin^2\theta_2\right)$$

Where;
$\mu = m/M$ = Ratio of the link mass (m) to tip mass (M)
L = Link length

BULLET: Jurnal Multidisiplin Ilmu
Volume 01, No. 03, Juni-Juli 2022
ISSN 2829-2049 (media online)
Hal 539-552

COMPUTED TORQUE CONTROL STRATEGY

Computed torque in its basic form means linearizing the feedback on as non-linear system. Computed torque control allows to derive effective robot controllers, while providing a framework to bring together classical independent joint control and some modern design techniques [5]. In this particular case, using computed torque control cancels the effects of gravitational, inertial and frictional forces of the robot. These forces are considered as disturbances and are removed at every joint while Lagrangian method is used to come up with dynamic equation to compute the rest of the forces [6].

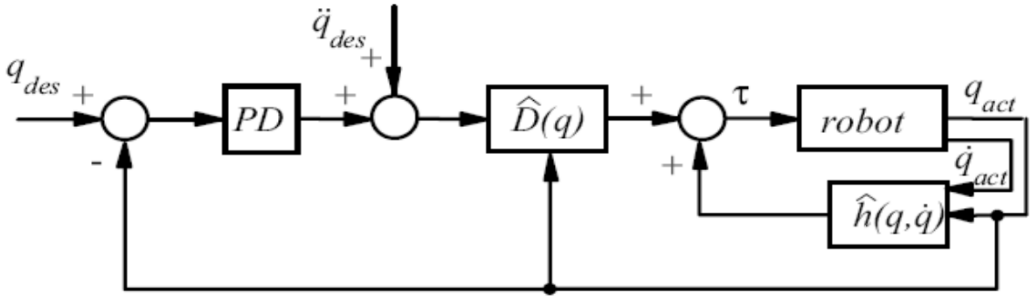

Figure 2: Strategy for Computed Torque Control [1]

Input to the computed torque controller is given by;

$$\begin{bmatrix} T_{1c} \\ T_{2c} \end{bmatrix} \equiv \widehat{\boldsymbol{D}} \begin{bmatrix} v_1 \\ v_2 \end{bmatrix} + \widehat{\boldsymbol{h}}(\boldsymbol{q}, \dot{\boldsymbol{q}})$$

Expatiating above equation yields;

$$\begin{bmatrix} T_{1c} \\ T_{2c} \end{bmatrix} \equiv \begin{bmatrix} I_{11} + I_{12} & I_{12} \\ I_{21} + I_{22} & I_{22} \end{bmatrix} \begin{bmatrix} v_1 \\ v_2 \end{bmatrix} + (m_2 L_{2cg} + M L_2) L_1 \sin(\theta_2) \begin{bmatrix} \omega_1^2 - \omega_2^2 \\ \omega_1^2 \end{bmatrix} + g \begin{bmatrix} \Gamma_1 \\ \Gamma_2 \end{bmatrix}$$

$q_{des}^T = [\theta_{1des} \quad \theta_{2des}]$ is given as the demand angular position commands to the joint servo motors. Therefore, substituting it into the above equation yields;

$$\begin{bmatrix} \ddot{\theta}_{1des} \\ \ddot{\theta}_{2des} \end{bmatrix} - \begin{bmatrix} \ddot{\theta}_1 \\ \ddot{\theta}_2 \end{bmatrix} + 2\omega_n \begin{bmatrix} \dot{\theta}_{1des} \\ \dot{\theta}_{2des} \end{bmatrix} - 2\omega_n \begin{bmatrix} \dot{\theta}_1 \\ \dot{\theta}_2 \end{bmatrix} + \omega_n^2 \begin{bmatrix} \theta_{1des} \\ \theta_{2des} \end{bmatrix} - \omega_n^2 \begin{bmatrix} \theta_1 \\ \theta_2 \end{bmatrix} = \begin{bmatrix} 0 \\ 0 \end{bmatrix}$$

$$\begin{bmatrix} T_1 \\ T_2 \end{bmatrix} = \begin{bmatrix} T_{1c} \\ T_{2c} \end{bmatrix} + \begin{bmatrix} \Delta T_1 \\ \Delta T_2 \end{bmatrix}$$

$$\begin{bmatrix} \Delta T_1 \\ \Delta T_2 \end{bmatrix} = \begin{bmatrix} I_{11} & I_{12} \\ I_{21} & I_{22} \end{bmatrix} \begin{bmatrix} \dot{\omega}_1 \\ \dot{\omega}_2 \end{bmatrix} - \begin{bmatrix} I_{11} + I_{12} & I_{12} \\ I_{12} + I_{22} & I_{22} \end{bmatrix} \begin{bmatrix} v_1 \\ v_2 \end{bmatrix}$$

Where $\dot{\omega}_1 = \ddot{\theta}_1$ and $\dot{\omega}_2 = \ddot{\theta}_1 + \ddot{\theta}_2$. Therefore;

$$\begin{bmatrix} \Delta T_1 \\ \Delta T_2 \end{bmatrix} = \left(\begin{bmatrix} I_{11} + I_{12} & I_{12} \\ I_{21} + I_{22} & I_{22} \end{bmatrix} - \begin{bmatrix} I_{12} & 0 \\ I_{22} & 0 \end{bmatrix} \right) \begin{bmatrix} \ddot{\theta}_1 \\ \ddot{\theta}_1 + \ddot{\theta}_2 \end{bmatrix} - \begin{bmatrix} I_{11} + I_{12} & I_{12} \\ I_{12} + I_{22} & I_{22} \end{bmatrix} \begin{bmatrix} v_1 \\ v_2 \end{bmatrix}$$

$$\begin{bmatrix} \Delta T_1 \\ \Delta T_2 \end{bmatrix} = \begin{bmatrix} I_{11} + I_{12} & I_{12} \\ I_{21} + I_{22} & I_{22} \end{bmatrix} \left(\begin{bmatrix} \ddot{\theta}_1 \\ \ddot{\theta}_2 \end{bmatrix} - \begin{bmatrix} v_1 \\ v_2 \end{bmatrix} \right)$$

$$\begin{bmatrix} v_1 \\ v_2 \end{bmatrix} = \begin{bmatrix} \ddot{\theta}_{1des} \\ \ddot{\theta}_{2des} \end{bmatrix} + 2\omega_n \left(\begin{bmatrix} \dot{\theta}_{1des} \\ \dot{\theta}_{2des} \end{bmatrix} - \begin{bmatrix} \dot{\theta}_1 \\ \dot{\theta}_2 \end{bmatrix} \right) + {\omega_n}^2 \left(\begin{bmatrix} \theta_{1des} \\ \theta_{2des} \end{bmatrix} - \begin{bmatrix} \theta_1 \\ \theta_2 \end{bmatrix} \right)$$

$$\begin{bmatrix} \Delta T_1 \\ \Delta T_2 \end{bmatrix} = \begin{bmatrix} I_{11} + I_{12} & I_{12} \\ I_{21} + I_{22} & I_{22} \end{bmatrix} \left(\begin{bmatrix} \ddot{\theta}_1 \\ \ddot{\theta}_2 \end{bmatrix} - \begin{bmatrix} \ddot{\theta}_{1d} \\ \ddot{\theta}_{2d} \end{bmatrix} + 2\omega_n \left(\begin{bmatrix} \dot{\theta}_{1d} \\ \dot{\theta}_{2d} \end{bmatrix} - \begin{bmatrix} \dot{\theta}_1 \\ \dot{\theta}_2 \end{bmatrix} \right) + {\omega_n}^2 \left(\begin{bmatrix} \theta_{1d} \\ \theta_{2d} \end{bmatrix} - \begin{bmatrix} \theta_1 \\ \theta_2 \end{bmatrix} \right) \right)$$

Tracking error = $\begin{bmatrix} e_1 \\ e_2 \end{bmatrix} = q_{des} - q_{act} = \begin{bmatrix} \theta_{1des} \\ \theta_{2des} \end{bmatrix} - \begin{bmatrix} \theta_1 \\ \theta_2 \end{bmatrix}$

BULLET: Jurnal Multidisiplin Ilmu
Volume 01, No. 03, Juni-Juli 2022
ISSN 2829-2049 (media online)
Hal 539-552

$$\begin{bmatrix}\Delta T_1\\ \Delta T_2\end{bmatrix} = \begin{bmatrix}I_{11}+I_{12} & I_{12}\\ I_{21}+I_{22} & I_{22}\end{bmatrix}\left(\begin{bmatrix}\ddot{e}_1\\ \ddot{e}_2\end{bmatrix} + 2\omega_n\begin{bmatrix}\dot{e}_1\\ \dot{e}_2\end{bmatrix} + {\omega_n}^2\begin{bmatrix}e_1\\ e_2\end{bmatrix}\right)$$

$$\begin{bmatrix}\ddot{e}_1\\ \ddot{e}_2\end{bmatrix} + 2\omega_n\begin{bmatrix}\dot{e}_1\\ \dot{e}_2\end{bmatrix} + {\omega_n}^2\begin{bmatrix}e_1\\ e_2\end{bmatrix} = \begin{bmatrix}I_{11}+I_{12} & I_{12}\\ I_{21}+I_{22} & I_{22}\end{bmatrix}^{-1}\begin{bmatrix}\Delta T_1\\ \Delta T_2\end{bmatrix}$$

$$\begin{bmatrix}\Delta T_1\\ \Delta T_2\end{bmatrix} = \begin{bmatrix}T_1\\ T_2\end{bmatrix} - \begin{bmatrix}T_{1c}\\ T_{2c}\end{bmatrix}$$

$$\begin{bmatrix}\ddot{e}_1\\ \ddot{e}_2\end{bmatrix} = 2\omega_n\begin{bmatrix}\dot{e}_1\\ \dot{e}_2\end{bmatrix} + \omega_n^2\begin{bmatrix}e_1\\ e_2\end{bmatrix} = \begin{bmatrix}0\\ 0\end{bmatrix}$$

DERIVATION OF KINETIC AND POTENTAL ENERGY

Y_1 is taken to be the height of the center of gravity of first link from the axis of first joint. Y_2 is the height of the center of gravity of the second link [7].

$$Y_1 = L_{1cg}sin\theta_1$$
$$Y_2 = L_1sin\theta_1 + L_{2cg}\sin(\theta_2+\theta_1)$$

For tip;

$$Y_T = L_1sin\theta_1 + L_2\sin(\theta_2+\theta_1)$$

Vertical velocities are given by;

$$\dot{Y}_1 = -L_{1cg}\dot{\theta}_1cos\theta_1$$
$$\dot{Y}_2 = -L_1\dot{\theta}_1cos\theta_1 + L_{2cg}(\dot{\theta}_2+\dot{\theta}_1)\cos(\theta_2+\theta_1)$$
$$\dot{Y}_T = -L_1\dot{\theta}_1cos\theta_1 + L_2(\dot{\theta}_2+\dot{\theta}_1)\cos(\theta_2+\theta_1)$$

Horizontal position of the center of gravity of the first and second links is given by;

$$X_1 = L_{1cg}cos\theta_1$$
$$X_2 = L_1cos\theta_1 + L_{2cg}\cos(\theta_2+\theta_1)$$
$$X_T = L_1cos\theta_1 + L_2\cos(\theta_2+\theta_1)$$

Horizontal velocities are thus;

$$\dot{X}_1 = -L_{1cg}\dot{\theta}_1sin\theta_1$$
$$\dot{X}_2 = -L_1\dot{\theta}_1sin\theta_1 - L_{2cg}(\dot{\theta}_2+\dot{\theta}_1)\sin(\theta_2+\theta_1)$$
$$\dot{X}_T = -L_1\dot{\theta}_1sin\theta_1 - L_2(\dot{\theta}_2+\dot{\theta}_1)\sin(\theta_2+\theta_1)$$

Change/increase of the potential energy of the system is given by;

$$V = g\sum_{i=1}^{n} m_iY_i$$

$$V = m_1g\left[L_{1cg}sin\theta_1\right] + m_2g\left[L_1sin\theta_1 + L_{2cg}\sin(\theta_1+\theta_2)\right] + Mg[L_1sin\theta_1 + L_2\sin(\theta_2+\theta_1)$$

$$= g(m_1L_{1cg} + m_2L_1 + ML_1)sin\theta_1 + g(m_2L_2 + ML_2)\sin(\theta_1+\theta_2)$$

Simplifying gives;

$$V = g\Gamma_{11}sin\theta_1 + g\Gamma_{22}\sin(\theta_1+\theta_2)$$

Where;

$$\Gamma_{11} = m_1L_{1c} + m_2L_1 + ML_1$$

$$\Gamma_{21} = m_2L_{2c} + ML_2$$

Following equation is used to derive the translational kinetic energy;

$$T_1 = \frac{1}{2}\sum_{i=1}^{n} m_i(\dot{X}_i^2 + \dot{Y}_i^2)$$

The kinetic energy of each component is;

$$T_1 = \frac{1}{2}m_1(\dot{X}_1^2 + \dot{Y}_1^2) + \frac{1}{2}m_2(\dot{X}_2^2 + \dot{Y}_2^2) + \frac{1}{2}M(\dot{X}_{tip}^2 + \dot{Y}_{tip}^2)$$

BULLET: Jurnal Multidisiplin Ilmu
Volume 01, No. 03, Juni-Juli 2022
ISSN 2829-2049 (media online)
Hal 539-552

$$= \frac{1}{2}m_1L_{1cg}^2\dot{\theta}_1^2 + \frac{1}{2}m_2(L_1^2\dot{\theta}_1^2 + L_{2cg}^2(\dot{\theta}_1+\dot{\theta}_2) + \frac{1}{2}M\left(L_1^2\dot{\theta}_1^2 + L_2^2(\dot{\theta}_1+\dot{\theta}_2)^2\right)$$
$$+ \left(m_2L_{2cg} + ML_2\right)L_1cos\theta_2\left(\dot{\theta}_1(\dot{\theta}_1+\dot{\theta}_2)\right)$$

The kinetic energy of the rotation of the rod is;

$$T_2 = \frac{1}{2}m_1k_1^2\dot{\theta}_1^2 + \frac{1}{2}m_2k_2^2(\dot{\theta}_1+\dot{\theta}_2)$$

Total kinetic = $T = T_1 + T_2$
Therefore;

$$T = \frac{1}{2}\left(m_1\left(L_{1cg}^2 + k_1^2\right) + (m_2+M)L_1^2\right)\theta_1^2 + \frac{1}{2}\left(m_2\left(L_{2cg}^2 + k_2^2\right) + ML_2^2\right)(\dot{\theta}_1+\dot{\theta}_2)^2$$
$$+ \left(m_2L_{2cg} + ML_2\right)(L_1cos\theta_2\left(\dot{\theta}_1(\dot{\theta}_1+\dot{\theta}_2)\right)$$

$$T = \frac{1}{2}I_{11}\dot{\theta}_1^2 + \frac{1}{2}I_{22}(\dot{\theta}_1+\dot{\theta}_2)^2 + I_{21}\dot{\theta}_1(\dot{\theta}_1+\dot{\theta}_2)$$

Where;

$$I_{11} = m_1\left(L_{1cg}^2 + k_{1cg}^2\right) + m_2L_1^2 + m_2L_{2cg}L_1\cos(\theta_2)$$
$$I_{21} = m_2L_{2cg}L_1\cos(\theta_2)$$
$$I_{22} = m_2\left(L_{2cg}^2 + k_{2cg}^2\right)$$

LAGRANGIAN APPROACH

Lagrangian approach is used to derive state-space representation of the system. Lagrangian approach uses the principle of the difference of kinetic and potential energy [8]. It is given by;

$L = K - P$ (1.1)

Euler-Lagrange equation is given by;

$$\frac{d}{dt}\frac{\partial L}{\partial \dot{q}_i} - \frac{\partial L}{\partial q_i} = Q_i \quad (1.2)$$

The equation below is simply formed using equation 1.1.

$$L = \frac{1}{2}I_{11}\dot{\theta}_1^2 + \frac{1}{2}I_{22}(\dot{\theta}_1+\dot{\theta}_2)^2 + I_{21}\dot{\theta}_1(\dot{\theta}_1+\dot{\theta}_2) - g\Gamma_{11}sin\theta_1 + g\Gamma_{22}\sin(\theta_1+\theta_2)$$

This will now enable to derive using Euler-Lagrange equation (1.2);

$$\frac{\partial L}{\partial \dot{q}_1} = I_{11}\dot{\theta}_1 + I_{12}(\dot{\theta}_1+\dot{\theta}_2)$$

$$\frac{\partial L}{\partial \dot{q}_2} = I_{21}\dot{\theta}_1 + I_{22}(\dot{\theta}_1+\dot{\theta}_2)$$

$$\frac{\partial L}{\partial q_1} = -g\Gamma_1$$

$$\frac{\partial L}{\partial q_2} = -g\Gamma_2 + \left(m_2L_{2cg} + ML_2\right)L_1sin\theta_2\left(\dot{\theta}_1(\dot{\theta}_1+\dot{\theta}_2)\right)$$

Where;

$$\Gamma_1 = \left(m_1L_{1cg} + m_2L_1 + ML_1\right)\cos(\theta_1) + \left(m_2L_{2cg} + ML_2\right)\cos(\theta_1+\theta_2)$$
$$\Gamma_2 = \left(m_2L_{2cg} + ML_2\right)\cos(\theta_1+\theta_2)$$

Therefore the Euler-Lagrange equations of motion can be expressed as:

BULLET: Jurnal Multidisiplin Ilmu
Volume 01, No. 03, Juni-Juli 2022
ISSN 2829-2049 (media online)
Hal 539-552

$$\begin{bmatrix} I_{11} & I_{12} \\ I_{21} & I_{22} \end{bmatrix}\begin{bmatrix} \ddot{\theta}_1 \\ \ddot{\theta}_1 + \ddot{\theta}_2 \end{bmatrix} + \begin{bmatrix} \dot{I}_{11} & \dot{I}_{12} \\ \dot{I}_{21} & \dot{I}_{22} \end{bmatrix}\begin{bmatrix} \dot{\theta}_1 \\ \dot{\theta}_1 + \dot{\theta}_2 \end{bmatrix} + \left(m_2 L_{2cg} + ML_2\right)L_1 sin\theta_2 \left(\dot{\theta}_1\left(\dot{\theta}_1 + \dot{\theta}_2\right)\right)\begin{bmatrix} 0 \\ 1 \end{bmatrix} + g\begin{bmatrix} \Gamma_1 \\ \Gamma_2 \end{bmatrix} = \begin{bmatrix} T_1 \\ T_2 \end{bmatrix}$$

Differentiating inertia expression with respect to time inertia gives;

$$\dot{\theta}_1 = \omega_1, \qquad \dot{\theta}_2 = \omega_2 - \omega_1$$

$$\begin{bmatrix} I_{11} & I_{12} \\ I_{21} & I_{22} \end{bmatrix}\begin{bmatrix} \dot{\omega}_1 \\ \dot{\omega}_2 \end{bmatrix} + \left(m_2 L_{2cg} + ML_2\right)L_1 sin\theta_2 \begin{bmatrix} \omega_1^2 - \omega_2^2 \\ \omega_1^2 \end{bmatrix} + g\begin{bmatrix} \Gamma_1 \\ \Gamma_2 \end{bmatrix} = \begin{bmatrix} T_1 \\ T_2 \end{bmatrix}$$

Where;

$$\Gamma_1 = \Gamma_{11}\cos(\theta_1) + \Gamma_{22}\cos(\theta_1 + \theta_2)$$

$$\Gamma_2 = \Gamma_{22}\cos(\theta_1 + \theta_2)$$

SIMULATION

DELTA-INVERSE SUB-SYSTEM

Figure 3 shows Delta-Inverse Sub-System. The torque input to the robotic manipulator is the torque that it fed into the Delta-Inverse Sub-System i.e. T1 and T2. The output of this sub-system is the angular velocities of link 1 and 2 [9].

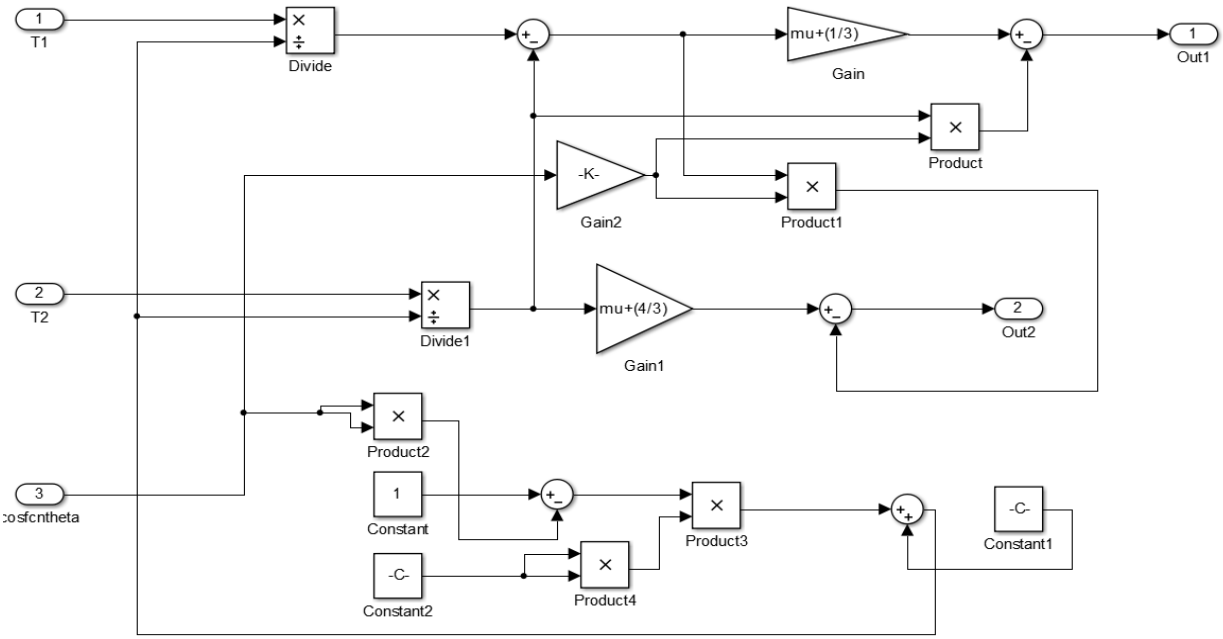

Figure 3: Delta-Inverse Sub-System

NON-DIMENSONAL TORQUE CONTROLLER

Motor control torque inputs is given by;

$$\begin{bmatrix} T_1 \\ T_2 \end{bmatrix} = \begin{bmatrix} T_{1c} \\ T_{2c} \end{bmatrix} = \begin{bmatrix} I_{11} + I_{12} & I_{12} \\ I_{21} + I_{22} & I_{22} \end{bmatrix}\begin{bmatrix} v_1 \\ v_2 \end{bmatrix} + \left(m_2 L_{2cg} + ML_2\right)L_1 \, sin\,\theta_2 \begin{bmatrix} \omega_1^2 - \omega_2^2 \\ \omega_1^2 \end{bmatrix}$$

$$I_{11} = m_1\left(L_{1cg}^2 + k_{1cg}^2\right) + \left(m_2 + M\right)L_1^2 + \left(m_2 L_{2cg} + ML_2\right)L_1\cos(\theta_2)$$

$$I_{11} = \left(\tfrac{1}{4} + \tfrac{1}{12}\right) + (1 + \mu) + \left(\tfrac{1}{2} + \mu\right)cos\theta_2 = \tfrac{4}{3} + \mu + \left(\tfrac{1}{2} + \mu\right)cos\theta_2$$

$$I_{12} = m_2\left(L_{2cg}^2 + k_{2cg}^2\right) + ML_2^2 + \left(m_2 L_{2cg} + ML_2\right)L_1\cos(\theta_2)$$

$$I_{12} = \left(\tfrac{1}{4} + \tfrac{1}{12}\right) + \mu + \left(\tfrac{1}{2} + \mu\right)cos\theta_2 = \tfrac{1}{3} + \mu + \left(\tfrac{1}{2} + \mu\right)cos\theta_2$$

BULLET: Jurnal Multidisiplin Ilmu
Volume 01, No. 03, Juni-Juli 2022
ISSN 2829-2049 (media online)
Hal 539-552

$$I_{21} = (m_2 L_{2cg} + ML_2) L_1 \cos(\theta_2)$$

$$I_{21} = \left(\frac{1}{2} + \mu\right) cos\theta_2$$

$$I_{22} = m_2(L_{2cg}^2 + k_{2cg}^2) + ML_2^2$$

$I_{22} = \left(\frac{1}{4} + \frac{1}{2}\right) + \mu = \frac{1}{3} + \mu$

Torque equations from which main Simulink diagram was constructed is given by;

$$T_1 = (I_{11} + I_{12})v_1 + I_{12}v_1 + \left(\frac{1}{2} + \mu\right) \sin(\theta_2)\,[\omega_1^1 - \omega_2^2]$$

$$T_2 = (I_{21} + I_{22})v_1 + I_{22}v_2 + \left(\frac{1}{2} + \mu\right) sin\theta_2[\omega_1^2]$$

$\dot{\theta}_1 = \omega_1 \leftrightarrow \omega_1^2 = \dot{\theta}_1^2,\ \dot{\theta}_2 = \omega_2 - \omega_1 \leftrightarrow -\dot{\theta}_2(\dot{\theta}_2 + 2\dot{\theta}_1)$

$$T_1 = \left[\frac{5}{3} + 2\mu + 2\left(\frac{1}{2} + \mu\right) cos\theta_2\right] v_1 + \left[\frac{1}{3} + \mu + \left(\frac{1}{2} + \mu\right) cos\theta_2\right] v_2 + \left[\left(\frac{1}{2} + \mu\right) sin\theta_2(-\dot{\theta}_2[\dot{\theta}_2 + 2\dot{\theta}_1])\right]$$

$$T_2 = \left[\frac{1}{3} + \mu + \left(\frac{1}{2} + \mu\right) cos\theta_2\right] v_1 + \left(\frac{1}{3} + \mu\right) v_2 + \left[\left(\frac{1}{2} + \mu\right) sin\theta_2(\dot{\theta}_1^2)\right]$$

$$\Delta(\mu)\begin{bmatrix}\dot{\omega}_1 \\ \dot{\omega}_2\end{bmatrix} = \begin{bmatrix}\mu + \frac{1}{3} & -\left(\mu + \frac{1}{3}\right) - \left(\mu + \frac{1}{2}\right) cos\theta_2 \\ -\left(\mu + \frac{1}{2}\right) cos\theta_2 & \mu + \frac{4}{3} + \left(\mu + \frac{1}{2}\right) cos\theta_2\end{bmatrix}\left[\begin{bmatrix}T_1/mL^2 \\ T_2/mL^2\end{bmatrix} - \left(\mu + \frac{1}{2}\right) sin\theta_2 \begin{bmatrix}\omega_1^2 - \omega_2^2 \\ \omega_1^2\end{bmatrix}\right]$$

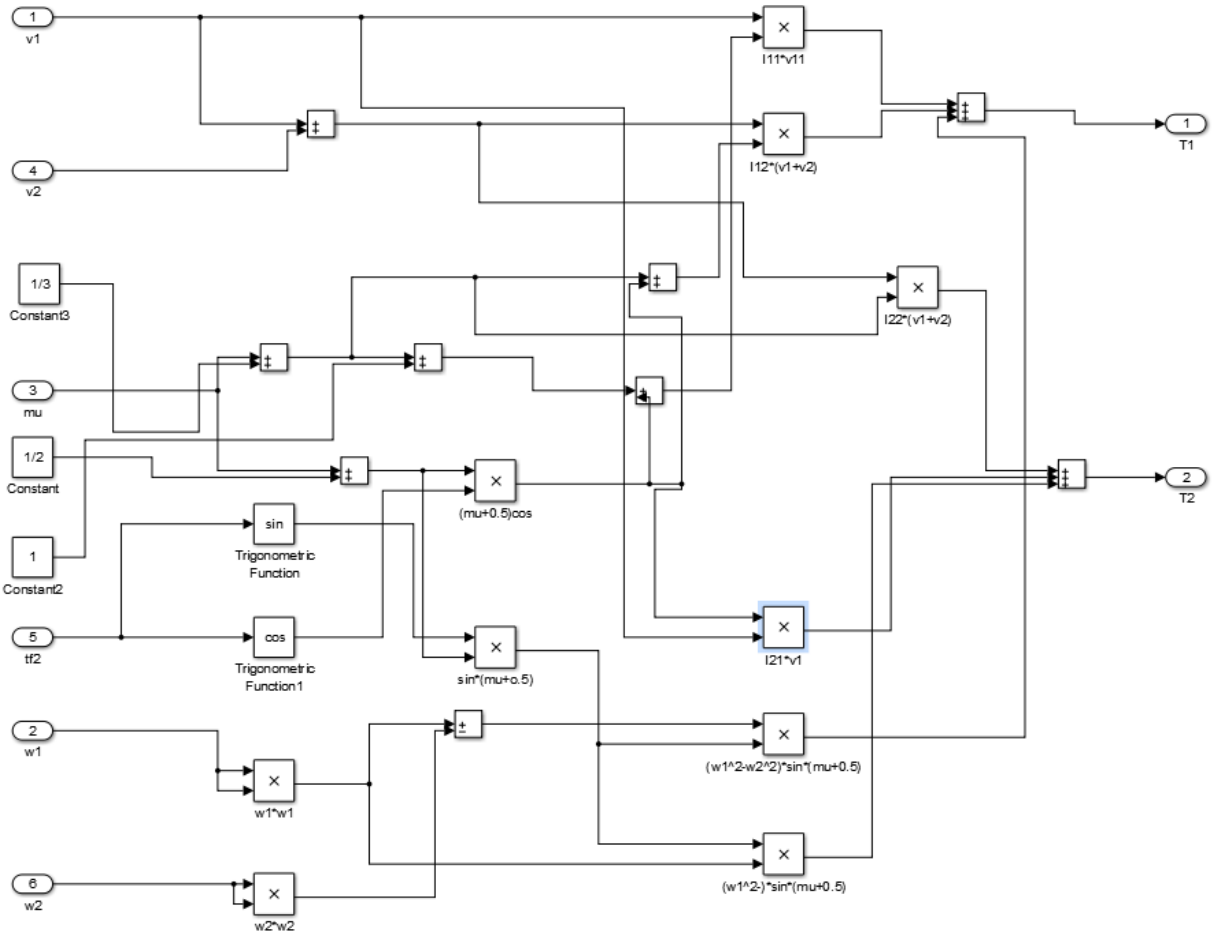

Figure 4: Non-Dimensional Torque Sub-System

The value for gravity g was set to zero and not included in the model as the gravity torques were assumed to be small.

BULLET: Jurnal Multidisiplin Ilmu
Volume 01, No. 03, Juni-Juli 2022
ISSN 2829-2049 (media online)
Hal 539-552

AUXILIARY CONTROL SUB-SYSTEM

Auxiliary control sub-system's equation is given by;

$$\begin{bmatrix} v_1 \\ v_2 \end{bmatrix} = \begin{bmatrix} \ddot{\theta}_{1des} \\ \ddot{\theta}_{2des} \end{bmatrix} + 2\omega_n \left(\begin{bmatrix} \dot{\theta}_{1des} \\ \dot{\theta}_{2des} \end{bmatrix} - \begin{bmatrix} \dot{\theta}_1 \\ \dot{\theta}_2 \end{bmatrix} \right) + {\omega_n}^2 \left(\begin{bmatrix} \theta_{1des} \\ \theta_{2des} \end{bmatrix} - \begin{bmatrix} \theta_1 \\ \theta_2 \end{bmatrix} \right)$$

Simulink model constructed from this equation is shown in figure 5. The input to the sub system is the desired angular acceleration, desired and actual feedback velocity, and the desired and actual feedback angular rotation [10]. The output of this subsystem is the error-compensated control acceleration and desired equation of motion for both links. The input and output of both links are the same [11].

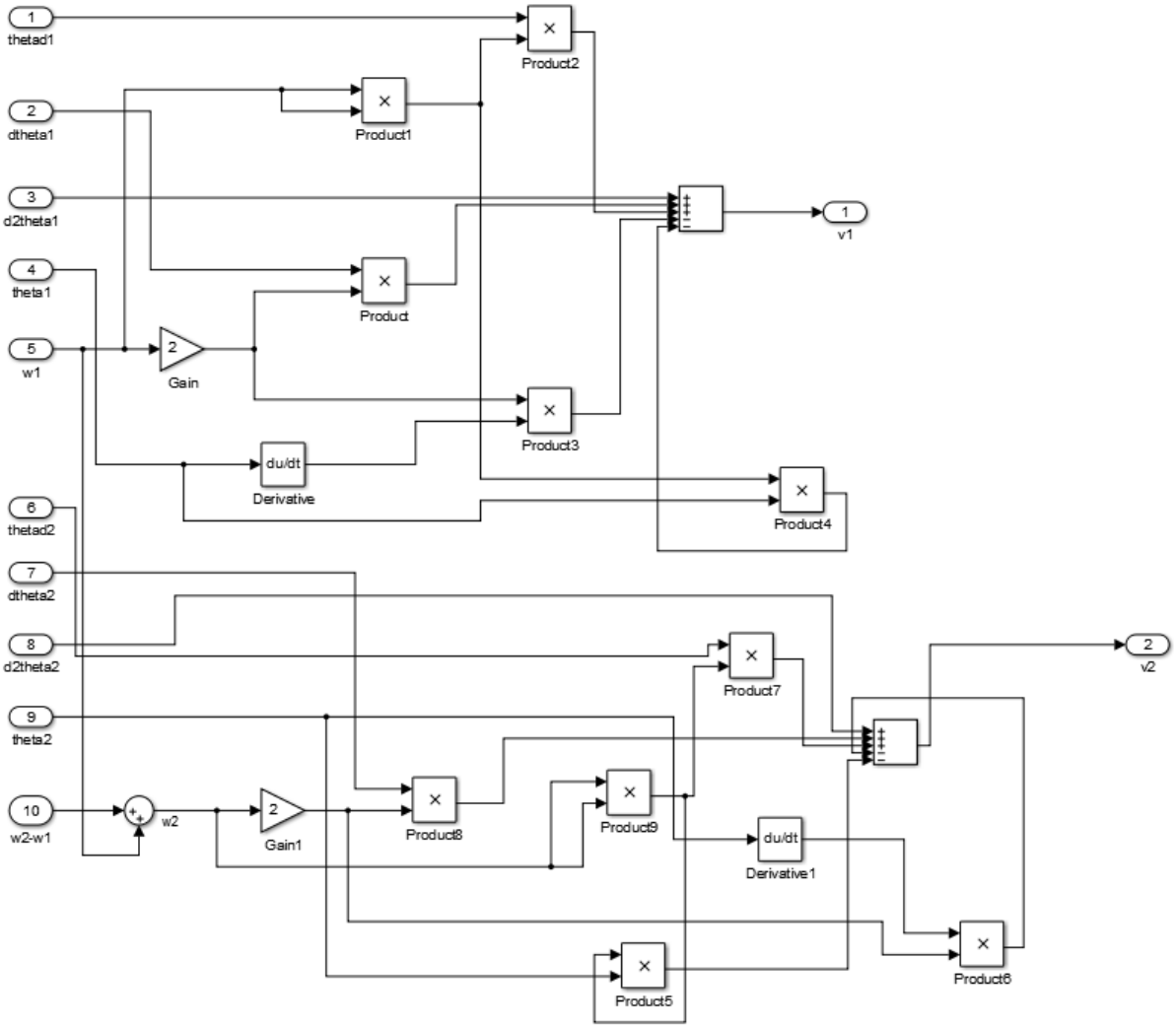

Figure 5: Auxiliary Control Sub-System

DEMAND SUB-SYSTEM

Equation for demand sub-system is;

$$\theta_d(t) = \theta_{d0}\left(1 - \exp\left(-\frac{t}{\tau}\right)\right), \tau\dot{\theta}_d + \theta_d = \theta_{d0}$$

Figure 6 shows the Simulink diagram constructed using the above equation;

BULLET: Jurnal Multidisiplin Ilmu
Volume 01, No. 03, Juni-Juli 2022
ISSN 2829-2049 (media online)
Hal 539-552

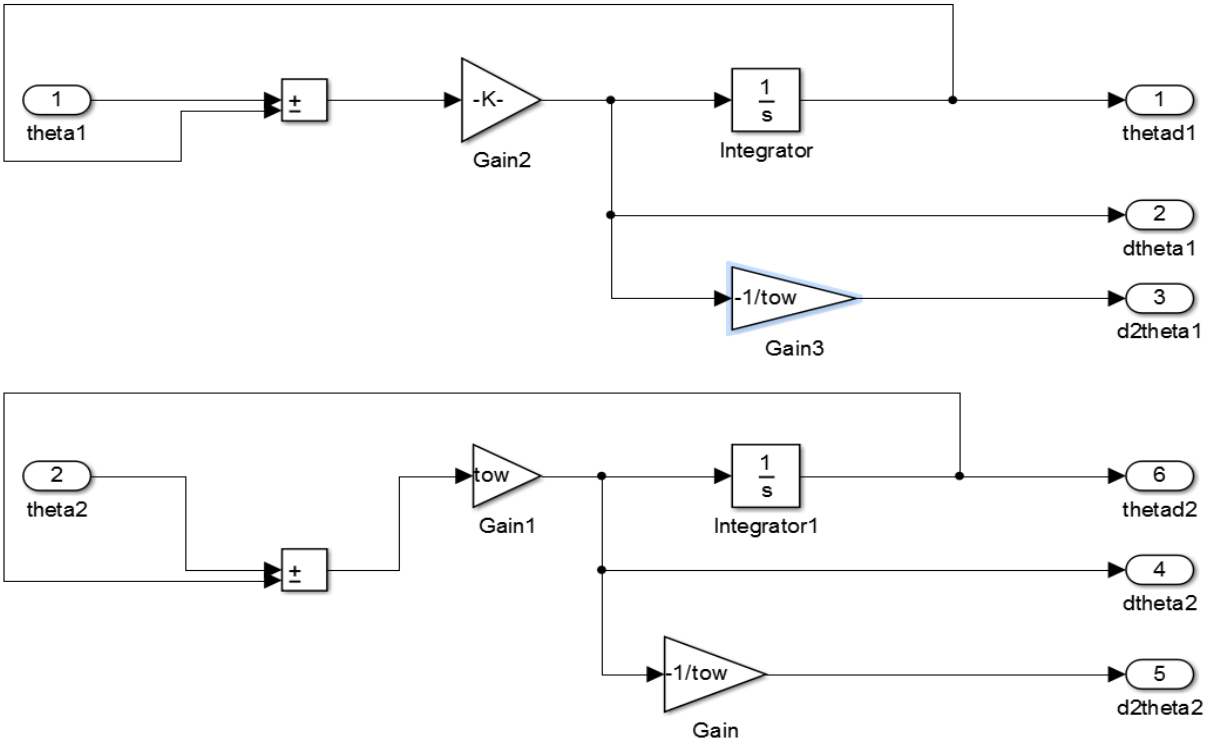

Figure 6: Demand Sub-System

BULLET: Jurnal Multidisiplin Ilmu
Volume 01, No. 03, Juni-Juli 2022
ISSN 2829-2049 (media online)
Hal 539-552

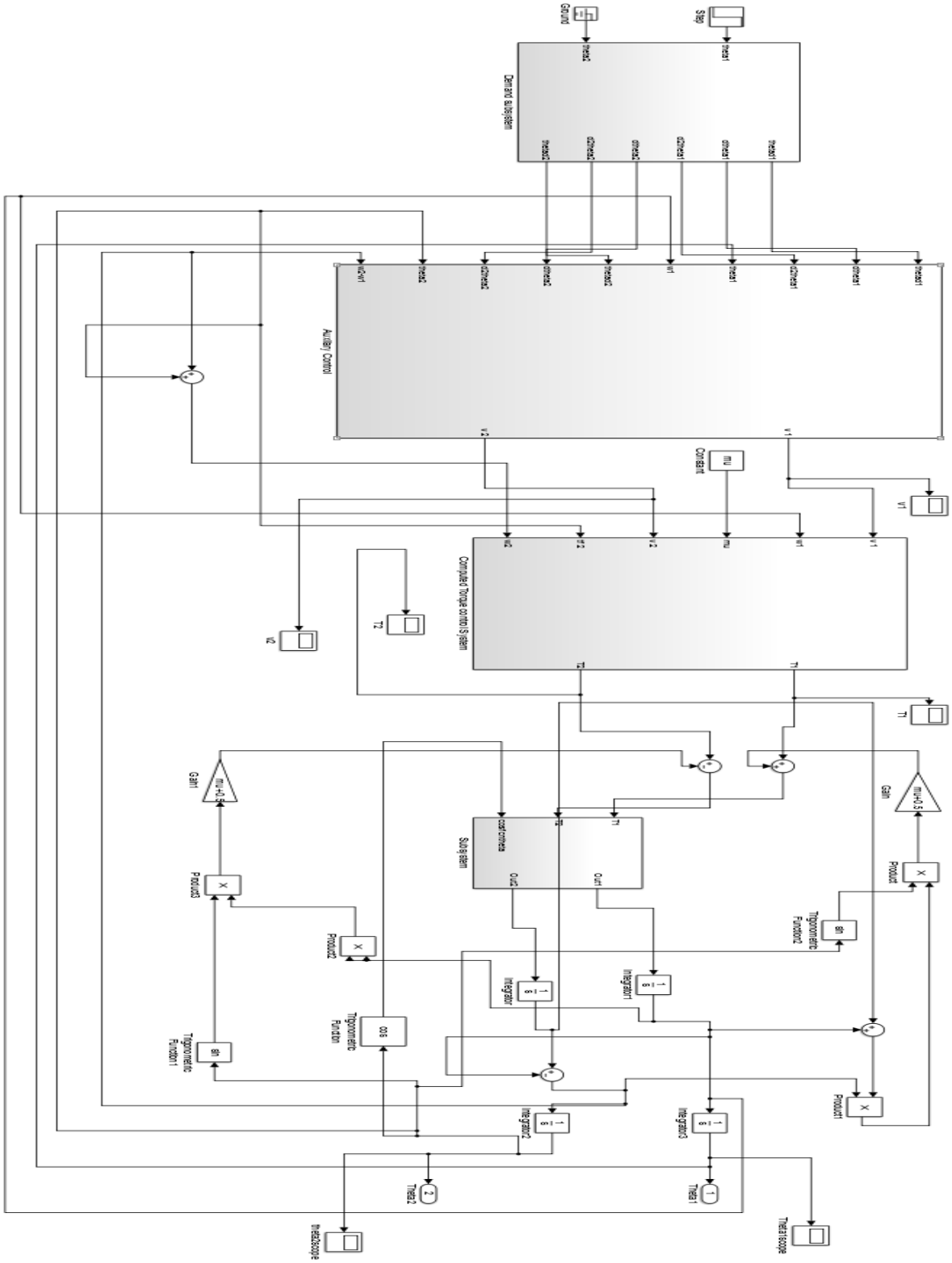

Figure 15: Complete System

BULLET: Jurnal Multidisiplin Ilmu
Volume 01, No. 03, Juni-Juli 2022
ISSN 2829-2049 (media online)
Hal 539-552

RESULTS

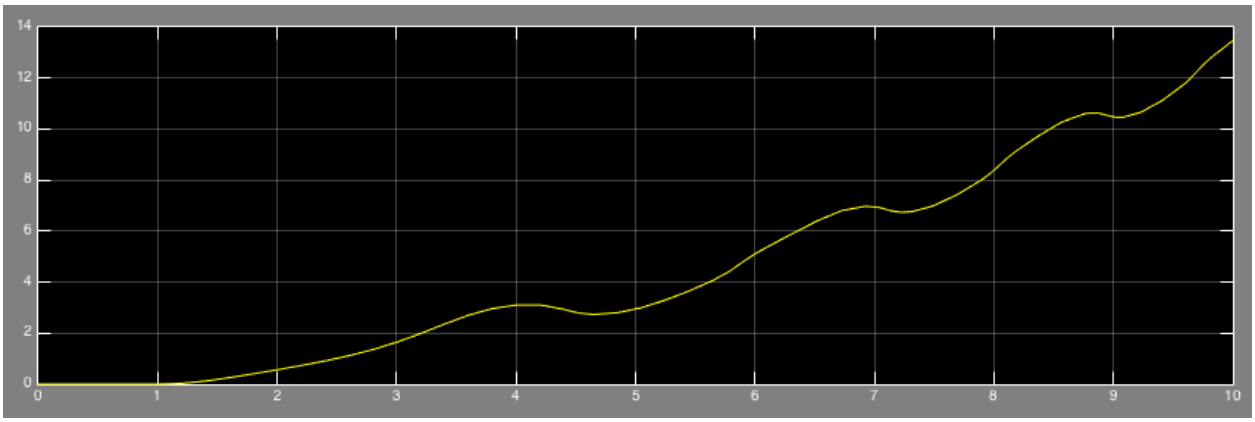

Figure 7: Initial Theta 1

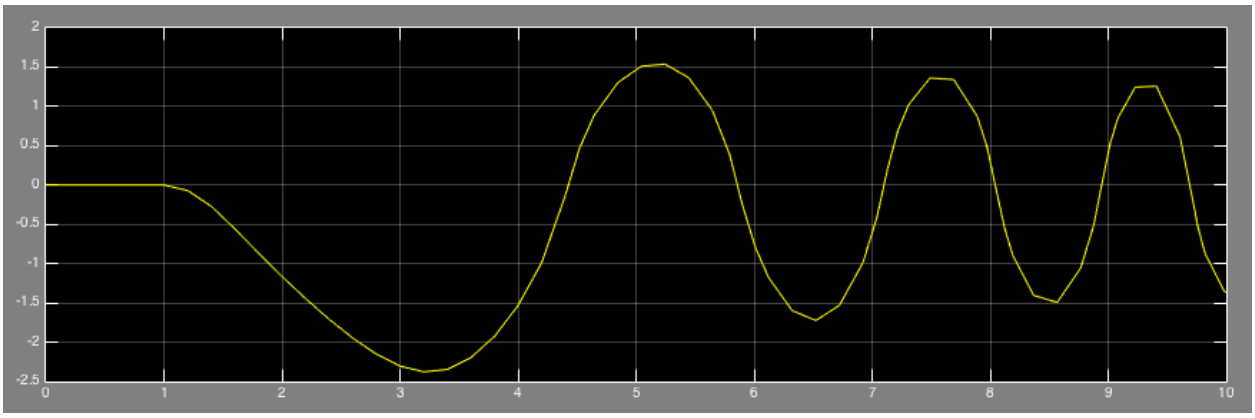

Figure 8: Initial Theta 2

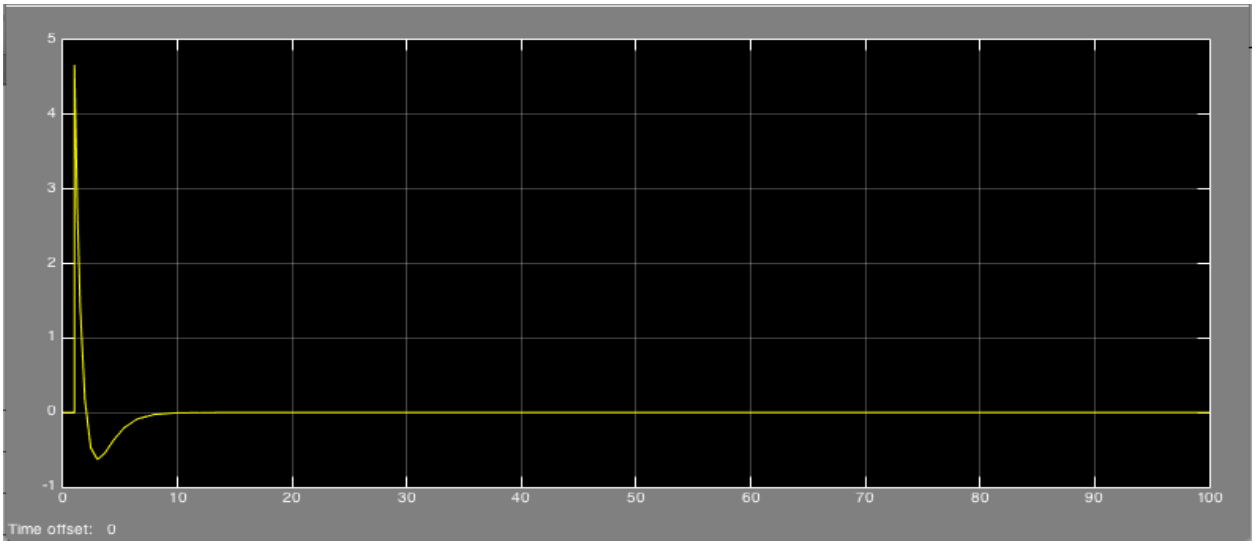

Figure 9: T1

BULLET: Jurnal Multidisiplin Ilmu
Volume 01, No. 03, Juni-Juli 2022
ISSN 2829-2049 (media online)
Hal 539-552

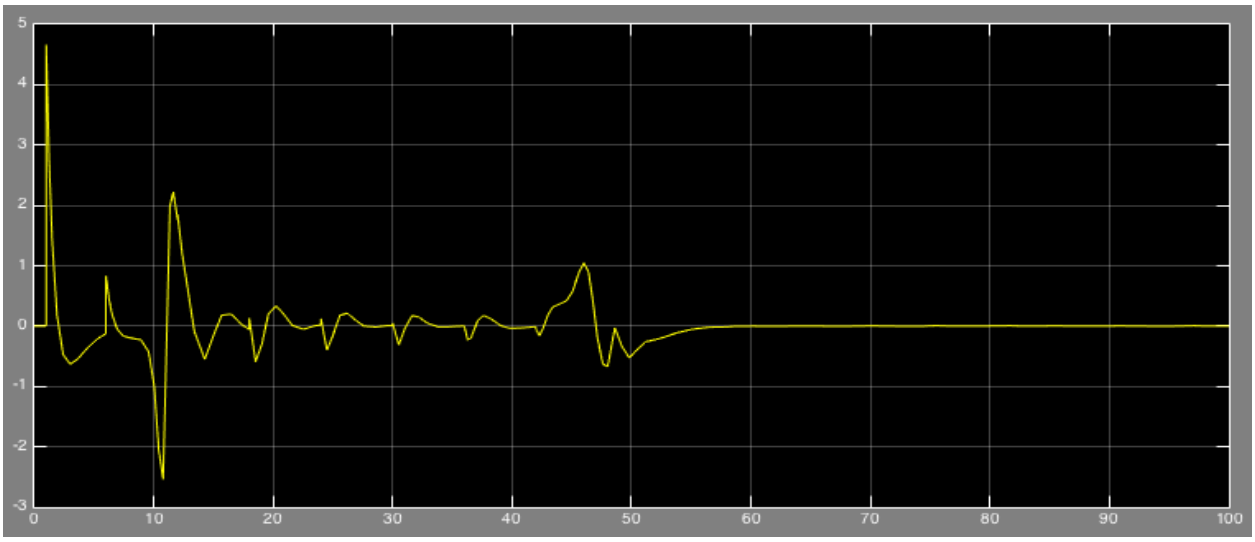

Figure 10: T1 8 steps

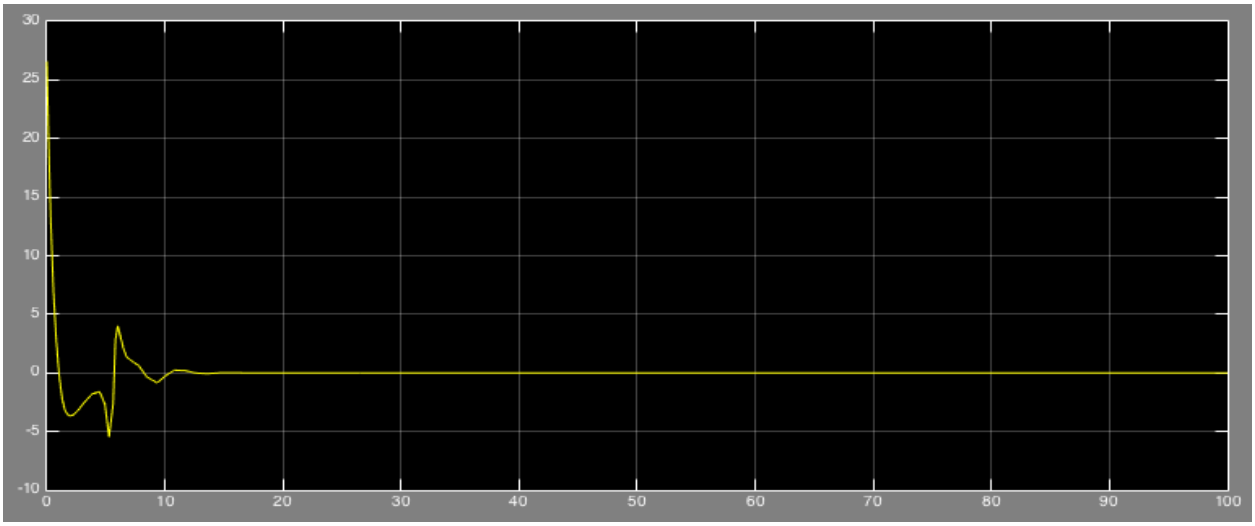

Figure 11: T1 Case2

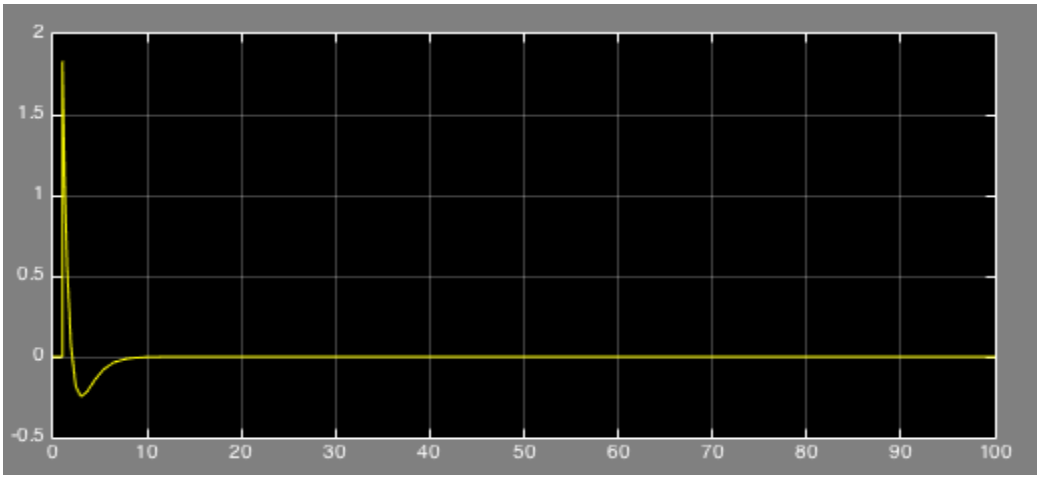

Figure 12: T2

BULLET: Jurnal Multidisiplin Ilmu
Volume 01, No. 03, Juni-Juli 2022
ISSN 2829-2049 (media online)
Hal 539-552

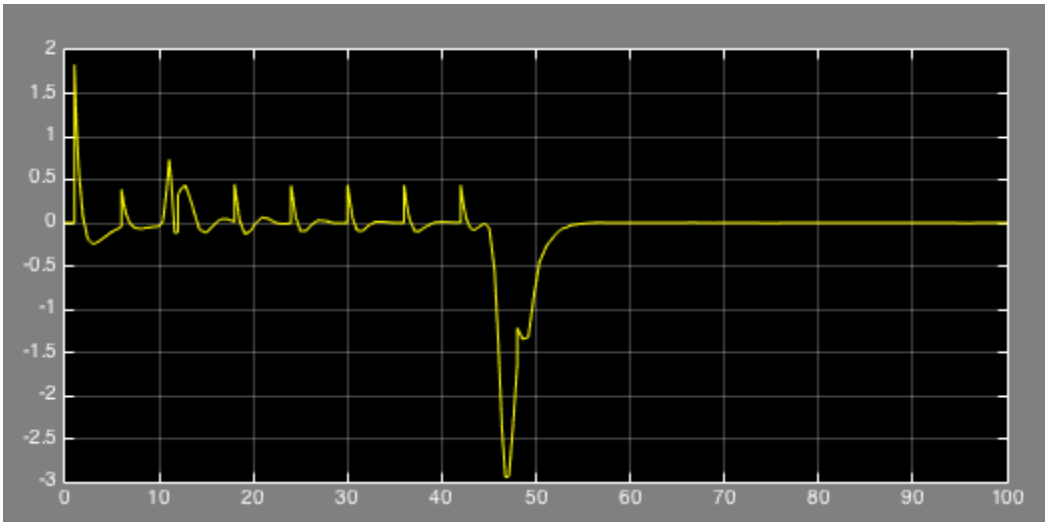

Figure 13: T2 8 Steps

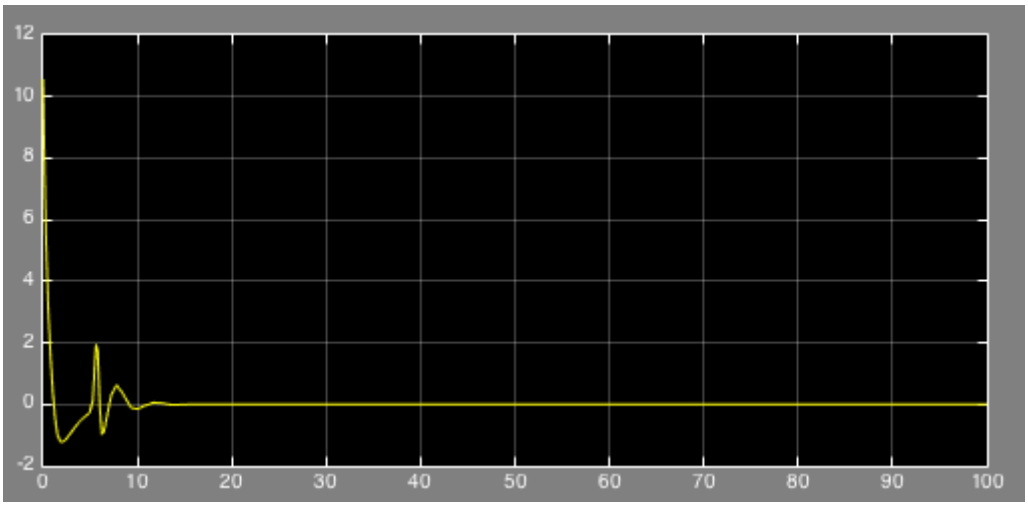

Figure 14: T2 Case 2

DISCUSSION

The two link planar anthropomorphic manipulator is modelled in Simulink using the initial conditions already given in the handout. Two links in the robotic arm is rotated in space about their respective joints when a torque is applied to them [12]. In order to measure the position of the link in space at every step, feedback is required to achieve the desired position. This feedback helps achieve the desired position by comparing the actual output with the desired value [13].

A simple system was first constructed with only the delta inverse subsystem included. The inputs were changed to a step function at T1 and ground function at T2. This is shown in figure 7 and figure 8. μ was taken to be 0.5. It can be sees that the signal for θ_1 is increasing whereas on the other hand the signal for θ_2 it is fluctuating [14].

Other control systems were added i.e. demand subsystem, auxiliary controls and the non-dimensional torque computer. Similarly, the tip mass of the system was altered in order to simulate the amount of torque acting on the inner and outer links. Reducing the tip load mass significantly reduced the torques acting on the link arms [15]. This is evident from the torque graphs for both methods of analysis that as the mass tip/link mass ratio increases, the torque input needed to reach the desired rotational position also increases. This may be due to a large moment of inertia caused by the increase in the mass of the tip [16].

Various parameters of the robotic arm is measured from the scopes that are attached to the sub-systems discussed earlier. A high torque is initially applied by the torque controller. It can also be thought of as a step response, where high input is given to achieve a desired position. A sharp decline in torque is seen that goes negative (below zero)

which is followed by a sharp rise until the system is stable back again [17]. This phenomena explains that velocity is increased initially as torque is applied but then as the torque is reduced, velocity reduces and becomes stable.

Concept of exponential decay has been established earlier in the report. Exponential decay acts as damping to the system. This is proved from quick stabilization of the system. It can be concluded here that the system has been successful in controlling the robotic manipulator. It is evident that the values obtained for the natural frequency governed the time taken for the link to reach its desired angle [18].

It is also evident that as the step size is increased, the accuracy of the results improve. This is because the model is solved at regular or more frequent intervals. However, increasing step size also increases the time computer takes to the run the simulation. Undershoot in many graphs is the proof that the system has errors. The manipulator is unable to handle the torque properly and thus many fluctuations are observed. The degrees of freedom of this manipulator limits the range of motion the arm can undergo. Moreover, increasing the tip mass will require more energy to be given to the system which might result in greater fluctuations [19]. In the Computed Torque Control Strategy section, it was discussed that gravitational, frictional and inertial forces are neglected. Since these forces are not included in the results, the actual torque required may be greater than it was required without considering disturbances [20].

CONCLUSIONS

Overall, it can be seen that the loops created were successful as the results gathered from it are smooth. The results show that different values of torque were achieved when the motion of inner and outer arm was changed. As expected, it was found that the torque increased with an increase in load at the tip mass. Also, increasing the step size to 8 ensured that lower torque forces were generated within the robot. However, this increased the overall completion time to the desired positions significantly.

REFERENCES

1. Computer Aided Simulation Tutorial Exercise 2015. Dr. R. Vepa. Queen Mary University of London.
2. Hošovský, A., Piteľ, J., Židek, K., Tóthová, M., Sárosi, J., & Cveticanin, L. (2016). Dynamic characterization and simulation of two-link soft robot arm with pneumatic muscles. *Mechanism and Machine Theory*, *103*, 98-116.
3. Suarez, A., Soria, P. R., Heredia, G., Arrue, B. C., & Ollero, A. (2017, September). Anthropomorphic, compliant and lightweight dual arm system for aerial manipulation. In *2017 IEEE/RSJ International Conference on Intelligent Robots and Systems (IROS)* (pp. 992-997). IEEE.
4. Wilson, J., Charest, M., & Dubay, R. (2016). Non-linear model predictive control schemes with application on a 2 link vertical robot manipulator. *Robotics and Computer-Integrated Manufacturing*, *41*, 23-30.
5. Ott, C., Eiberger, O., Friedl, W., Bauml, B., Hillenbrand, U., Borst, C., ... & Hirzinger, G. (2006, December). A humanoid two-arm system for dexterous manipulation. In *2006 6th IEEE-RAS international conference on humanoid robots* (pp. 276-283). IEEE.
6. Zaki, A. S., & ElMaraghy, W. H. (1992). Modelling and control of a two-link flexible manipulator. *Transactions of the Canadian Society for Mechanical Engineering*, *16*(3-4), 311-328.
7. Su, H., Qi, W., Yang, C., Aliverti, A., Ferrigno, G., & De Momi, E. (2019). Deep neural network approach in human-like redundancy optimization for anthropomorphic manipulators. *IEEE Access*, *7*, 124207-124216.
8. Klimchik, A., Wu, Y., Caro, S., & Pashkevich, A. (2011, July). Design of experiments for calibration of planar anthropomorphic manipulators. In *2011 IEEE/ASME International Conference on Advanced Intelligent Mechatronics (AIM)* (pp. 576-581). IEEE.
9. Sciavicco, L., & Siciliano, B. (2012). *Modelling and control of robot manipulators*. Springer Science & Business Media.
10. Caurin, G. A. D. P., Albuquerque, A. R. L., & Mirandola, A. L. D. A. (2004, September). Manipulation strategy for an anthropomorphic robotic hand. In *2004 IEEE/RSJ International Conference on Intelligent Robots and Systems (IROS)(IEEE Cat. No. 04CH37566)* (Vol. 2, pp. 1656-1661). IEEE.

11. Xu, Q., Li, Z., Li, H., Yu, X., & Yang, Y. (2024). ATDM: An Anthropomorphic Aerial Tendon-driven Manipulator with Low-Inertia and High-Stiffness. *arXiv preprint arXiv:2405.04821*.
12. Capisani, L. M., Facchinetti, T., Ferrara, A., & Martinelli, A. (2013). Obstacle modelling oriented to safe motion planning and control for planar rigid robot manipulators. *Journal of Intelligent & Robotic Systems*, *71*, 159-178.
13. Ma, R. R., & Dollar, A. M. (2014). Linkage-based analysis and optimization of an underactuated planar manipulator for in-hand manipulation. *Journal of Mechanisms and Robotics*, *6*(1), 011002.
14. Damic, V., & Cohodar, M. (2006). Bond graph based modelling and simulation of flexible robotic manipulators. In *Proceedings 20th European Conference on Modelling and Simulation, Editors: Wolfgang Borutzky, Alessandra Orsoni, Richard Zobel© ECMS*.
15. Mohammed Elawady, W., Bouteraa, Y., & Elmogy, A. (2020). An adaptive second order sliding mode inverse kinematics approach for serial kinematic chain robot manipulators. *Robotics*, *9*(1), 4.
16. Lau, D. T. M. (2014). *Modelling and analysis of anthropomorphic cable-driven robots* (Doctoral dissertation, University of Melbourne, Department of Mechanical Engineering).
17. Nishio, A., Takahashi, K., & Nenchev, D. N. (2006, October). Balance control of a humanoid robot based on the reaction null space method. In *2006 IEEE/RSJ International Conference on Intelligent Robots and Systems* (pp. 1996-2001). IEEE.
18. Ebrahimi, N. (2019). Simulation of a three link-Six Musculo Skeletal Arm Activated by Hill Muscle Model.
19. Tondu, B. (2005, December). Modelling of the shoulder complex and application the design of upper extremities for humanoid robots. In *5th IEEE-RAS International Conference on Humanoid Robots, 2005.* (pp. 313-320). IEEE.
20. Brambilla, D., Capisani, L. M., Ferrara, A., & Pisu, P. (2008). Fault detection for robot manipulators via second-order sliding modes. *IEEE Transactions on Industrial Electronics*, *55*(11), 3954-3963.